

## Magnetic properties and magnetic structures of $\text{Ho}_{1-x}\text{Y}_x\text{Ni}$ compounds

This content has been downloaded from IOPscience. Please scroll down to see the full text.

1995 J. Phys.: Condens. Matter 7 2843

(<http://iopscience.iop.org/0953-8984/7/14/021>)

View [the table of contents for this issue](#), or go to the [journal homepage](#) for more

Download details:

IP Address: 128.6.218.72

This content was downloaded on 06/09/2015 at 03:30

Please note that [terms and conditions apply](#).

## Magnetic properties and magnetic structures of $\text{Ho}_{1-x}\text{Y}_x\text{Ni}$ compounds

J A Blanco†, J Rodriguez Fernandez‡, J C Gómez Sal†, J Rodriguez-Carvajal§ and D Gignoux||

† Departamento de Física, Universidad de Oviedo, 33007 Oviedo, Spain

‡ Facultad de Ciencias, Universidad de Cantabria, 39005 Santander, Spain

§ Laboratoire Leon Brillouin (CEA-CNRS), Centre d'Etudes de Saclay, Gif sur Yvette, and Institut Laue–Langevin, France

|| Laboratoire Louis Néel, CNRS, 166X 38042, Grenoble, France

Received 28 September 1994, in final form 6 January 1995

**Abstract.** The magnetic properties of orthorhombic  $\text{Ho}_{1-x}\text{Y}_x\text{Ni}$  compounds have been studied from resistivity, magnetization and neutron diffraction experiments. The Curie temperatures decrease linearly from 37.5 K in  $\text{HoNi}$  to 4 K for  $\text{Ho}_{0.2}\text{Y}_{0.8}\text{Ni}$ , while  $\text{Ho}_{0.1}\text{Y}_{0.9}\text{Ni}$  and  $\text{YNi}$  do not present any magnetic long-range order. Below  $T_C$  the compounds show a non-collinear magnetic structure belonging to a single irreducible representation, which evolves at lower temperatures towards another non-collinear structure described by the mixture of two irreducible representations. The appearance of both magnetic arrangements is discussed, comparing these structures with those of other rare earth nickel compounds and taking into account both crystalline electric field and exchange interactions.

### 1. Introduction

Low-symmetry rare earth (RE) intermetallic systems are especially sensitive to the competition between magnetic exchange interactions and crystalline electric field (CEF) anisotropy. Among them, the equiatomic orthorhombic  $\text{RENi}$  compounds, where Ni is not magnetic, provide an excellent example of the influence of both mechanisms on the physical properties. In particular, the structure and magnetism of  $\text{HoNi}$  have been previously investigated by x-ray and neutron diffraction, magnetization and electrical resistivity using polycrystalline samples [1–4]. The thermal evolution of the magnetic structure of this compound was studied in further investigations by means of torque [5], magnetization [6] and neutron diffraction experiments [7] performed on single crystals.

$\text{HoNi}$  presents, below the Curie temperature  $T_C = 37$  K, a non-collinear structure with magnetic moments lying in the  $ac$  plane, while for temperatures lower than  $T_i = 15$  K, the magnetic ordering is also non-collinear, but a ferromagnetic component appears along the  $b$  direction [7].

In order to obtain a better insight into this low-temperature transition and analyse in detail the relative importance of CEF and magnetic interactions, we have considered it interesting to replace the holmium atoms by non-magnetic yttrium ones. This substitution mainly modifies the magnetic exchange interactions, having a minor influence of CEF effects. Therefore significant changes in the magnetic properties of the system are expected.

In this paper we present the results of resistivity (section 2), magnetization (section 3) and neutron diffraction experiments (section 4). The pseudobinary  $\text{Ho}_{1-x}\text{Y}_x\text{Ni}$  compounds,

which were prepared by melting Ho, Y and Ni in an induction furnace, crystallize in the same FeB-type orthorhombic structure ( $Pnma$  space group) as HoNi. The purity of the samples was checked by x-ray analysis. No supplementary phases have been found as far as the analysis permits.

## 2. Resistivity measurements

Resistivity was measured by means of the AC probe method, for temperatures ranging from 1.5 K to 300 K, at the Laboratorio de Física de la Materia Condensada de la Universidad de Cantabria. Figure 1 shows the thermal variation of the resistivity at low temperatures of the  $\text{Ho}_{1-x}\text{Y}_x\text{Ni}$  compounds investigated ( $x = 0, 0.2, 0.4, 0.6, 0.8, 0.9$  and 1). Changes in the slope of the  $\rho(T)$  curves at the Curie temperature,  $T_C$ , and at the intermediate phase transition temperature,  $T_I$  are observed and marked with arrows in figure 1. The values of these characteristic temperatures,  $T_C$  and  $T_I$ , are, respectively, 39.2 and 14.0 K for HoNi. Both temperatures decrease mostly linearly with the yttrium content and they are presented in table 1. For  $x = 0.8$ ,  $T_C = 4.6$  K and no intermediate magnetic phase was found down to 1.5 K, the lowest temperature measured. For  $x = 0.9$  and 1 we have not observed any magnetic order down to 1.5 K.

**Table 1.** Magnetic properties of  $\text{Ho}_{1-x}\text{Y}_x\text{Ni}$  compounds.  $T_C$ ,  $T_I$  and  $\theta_p$  are the Curie, the intermediate and the paramagnetic Curie temperatures.  $\mu_{\text{eff}}$  is the paramagnetic moment. The values of  $T_C$  and  $T_I$  correspond to the determination obtained from resistivity  $\rho_{\text{mag}}$  and magnetic  $M(H)$  measurements.

$x$	$T_C$ (K)		$T_I$ (K)		$\theta_p$ (K)	$\mu_{\text{eff}}$ ( $\mu_B/\text{Ho}$ )	Magnetization at 1.5 K and 80 kOe ( $\mu_B/\text{Ho}$ )
	$\rho_{\text{mag}}$	$M(H)$	$\rho_{\text{mag}}$	$M(H)$			
0	39.2	37.5	14.0	15.0	30	10.54	7.71
0.2	32.5	32.0	10.2	10.0	29	10.54	8.60
0.4	21.5	21.0	6.7	5.0	20	10.68	8.77
0.6	11.4	11.0	3.4	3.0	10	10.50	7.62
0.8	4.6	4.0	—	—	6	10.87	7.82
0.9	—	—	—	—	2	11.66	8.32

As occurs in other RENi compounds [8], the samples are very brittle and it is then a difficult task to obtain the correct values for the lattice,  $\rho_{\text{latt}}$ , and magnetic contributions,  $\rho_{\text{mag}}$ . However, we have estimated  $\rho_{\text{mag}}$  following the procedure explained in [9], which was useful for the determination of the magnetic resistivities of  $\text{GdNi}_{1-x}\text{Cu}_x$  [9] and  $\text{REPt}$  [10]. The lattice contribution of each  $\text{Ho}_{1-x}\text{Y}_x\text{Ni}$  compound was obtained from that of the non-magnetic YNi one, taking into account the mass correction. The  $\rho_{\text{mag}}$  curves obtained in this way are compared in figure 2. For all the compounds with magnetic order, the resistivity at temperatures higher than  $T_C$  is not constant but increases continuously, before reaching the spin disorder resistivity saturation value,  $\rho_{\text{sdr}}$ , around 140 K. This behaviour is related to the CEF effects on the resistivity and the saturation temperature gives an indication of the CEF splitting [11]. Therefore, this splitting seems to be mostly the same for all the studied compounds. However, the  $\rho_{\text{sdr}}$  value, which is directly related to the intensity of the magnetic interactions, decreases with increasing yttrium content.

In the ordered range the analysis of the magnetic resistivity leads to two potential behaviours as a function of temperature,  $\rho_{\text{mag}} \propto T^n$ . In the range  $(0, T_I)$  the exponent is

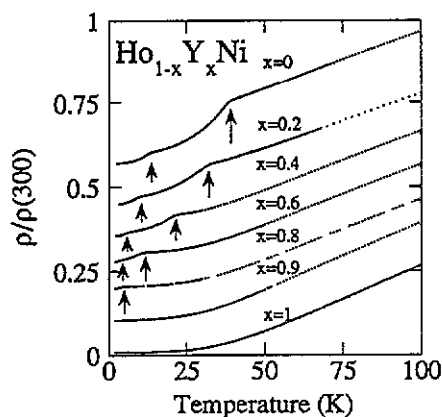


**Figure 1.** The thermal variation in the electrical resistivities of  $\text{Ho}_{1-x}\text{Y}_x\text{Ni}$  ( $x = 0, 0.2, 0.4, 0.6, 0.8, 0.9$  and  $1$ ). For  $\text{YNi}$  ( $x = 1$ ) circles represent experimental points and full lines Grüneisen-Bloch fitting (Debye temperature, 230 K). Arrows indicate the  $T_i$  and  $T_C$  temperatures.

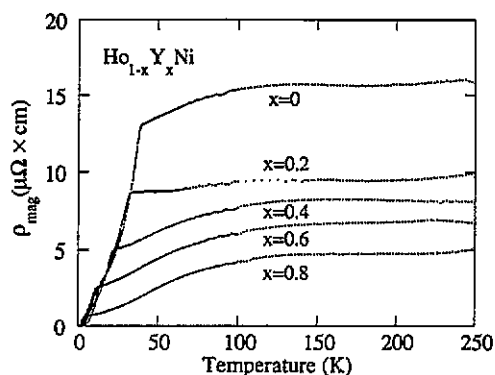


**Figure 2.** The thermal variation in the magnetic contribution to the resistivity of  $\text{Ho}_{1-x}\text{Y}_x\text{Ni}$  ( $x = 0, 0.2, 0.4, 0.6$  and  $0.8$ ).

mostly  $n = 3$  for all the compounds and in the interval  $(T_i, T_C)$  the exponent  $n$  decreases from  $n = 3$  for  $\text{HoNi}$  to  $n = 1$  for  $\text{Ho}_{0.2}\text{Y}_{0.8}\text{Ni}$ . In the absence of accurate theoretical models for the resistivity behaviour in the ordered range, considering both CEF and exchange interactions, we can only assert, in the same way as in previous papers [9, 12], that the different exponents depend on the ratio between CEF anisotropy and magnetic interactions. From all these experimental data we can deduce a rule that seems to be general: the highest exponents corresponds to the highest values of this ratio.

### 3. Magnetic properties

The bulk magnetic measurements were performed using the extraction method under magnetic fields of up to 80 kOe in the temperature range 1.5–300 K at the Laboratoire Louis Néel in Grenoble.

The thermal dependences of the reciprocal susceptibilities obtained from Arrot plots shows Curie-Weiss laws, at temperatures above 50 K, leading to paramagnetic effective magnetic moments quite close to that of the free  $\text{Ho}^{3+}$  ion,  $10.61\mu_B$ . The paramagnetic Curie temperature decreases as yttrium content  $x$  increases (see table 1), reaching the value of 2 K at  $x = 0.9$  for which no magnetic order is observed down to 1.5 K. The large value observed for  $x = 0.8$  and  $0.9$  is related to the Pauli temperature-independent contribution to the susceptibility arising from the conduction band.

Figure 3 shows the thermal dependences of the magnetization over magnetic field,  $M/H$ , in a constant magnetic field of 2 kOe for the compounds  $x = 0, 0.4$  and  $0.9$  as representative examples. These measurements confirm the existence of a transition  $T_i$ , below the Curie temperature  $T_C$ , already observed by resistivity measurements for all the compounds with  $x \leq 0.6$ . The values of the critical temperatures are taken at the inflexion point of the curves and are gathered in table 1. They agree quite well with those obtained from resistivity.

In figure 4 the Curie temperature,  $T_C$ , and the intermediate transition temperature,  $T_i$ , are represented as a function of the Y content. For the studied compounds, as commented

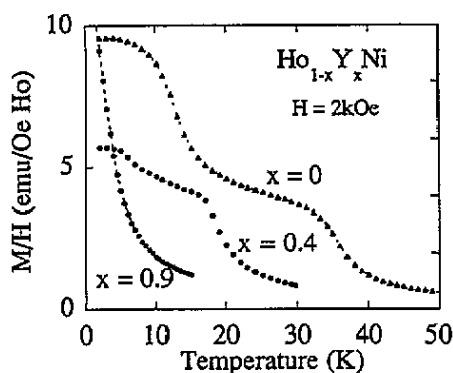


Figure 3. The thermal variation of the magnetization over the magnetic field,  $M/H$ , under a magnetic field  $H = 2$  kOe for  $\text{Ho}_{1-x}\text{Y}_x\text{Ni}$  compounds ( $x = 0, 0.4$  and  $0.9$ ).

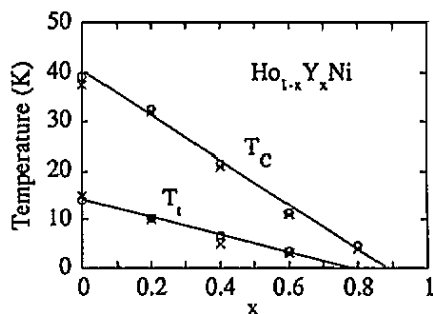


Figure 4. The dependence of the ordering temperature  $T_C$  and the intermediate ferromagnetic transition temperature  $T_I$  on the concentration  $x$  in  $\text{Ho}_{1-x}\text{Y}_x\text{Ni}$  compounds.

before in section 2, the substitution of Y ions for Ho, in the diluted  $\text{Ho}_{1-x}\text{Y}_x\text{Ni}$  compounds, depresses almost linearly the magnetic ordering temperature, which vanishes for a critical concentration value around  $x_c = 0.9$ . The low-temperature magnetic phase transition disappears for concentrations close to  $x = 0.8$ .

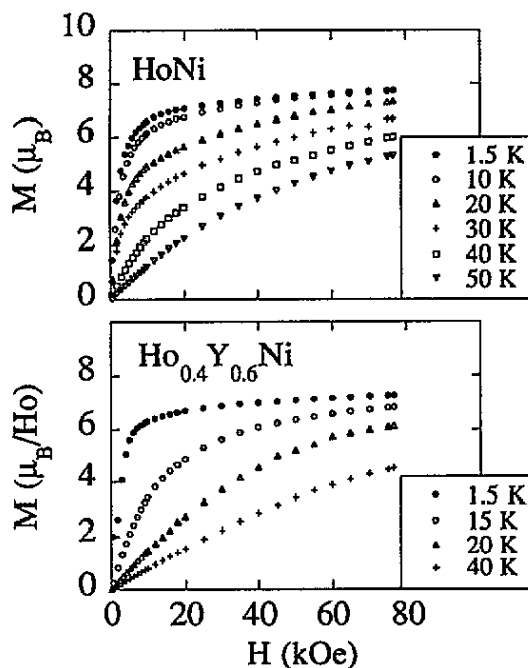


Figure 5. The magnetization curves of  $\text{HoNi}$  and  $\text{Ho}_{0.4}\text{Y}_{0.6}\text{Ni}$  compounds.

The isothermal magnetization curves are presented in figure 5 for  $\text{HoNi}$  and  $\text{Ho}_{0.4}\text{Y}_{0.6}\text{Ni}$ , as representative examples. At low temperatures, the saturation of the magnetization is

almost reached, being 7.7 and  $7.6\mu_{\text{B}}/\text{Ho}$  for  $x = 0$  and  $x = 0.6$  respectively. Due to the polycrystalline nature of the samples, the apparent erratic variation of the saturated magnetic moment as a function of the yttrium concentration is not significant and it is quite difficult to appreciate some differences between the isothermal magnetization curves in the region  $T_i < T < T_C$  and those measured in the interval  $1.5 \text{ K} < T < T_i$ . In both regions the curves are characteristic of a ferromagnetic behaviour.

#### 4. Magnetic structures

Neutron diffraction experiments were performed on the D1B diffractometer ( $\lambda = 2.51 \text{ \AA}$ ) of the high-flux reactor of the Institute Laue-Langevin in Grenoble for the compounds  $\text{Ho}_{1-x}\text{Y}_x\text{Ni}$  with  $x = 0, 0.2$  and  $0.6$ .

The analysis of the data was performed using the programs existing in the STRAP package [13]. The refinements of the crystal and magnetic structures were carried out using the program FULLPROF [14], based on the Rietveld method, where the full profile of the spectra is used to fit both the structural and magnetic models. As an example of the neutron patterns and the Rietveld refinements we present in figure 6 those obtained for  $\text{Ho}_{0.8}\text{Y}_{0.2}\text{Ni}$ .

The patterns in the paramagnetic phase were collected at 60, 40 and 20 K for  $x = 0, 0.2$  and  $0.6$ , respectively. All these patterns can be indexed in the orthorhombic system respecting the extinction conditions of the space group  $Pnma$  ( $((0, k, l), k + l = 2n$  and  $(h, 0, 0), h = 2n)$ ). The Ho/Y ions lie randomly distributed in a (4c) site, while Ni ions are also in a (4c) site with different atomic coordinates. The equivalent positions of such a site are

$$(1) (x, \frac{1}{4}, z) \quad (2) (-x, -\frac{1}{4}, -z) \quad (3) (\frac{1}{2} - x, -\frac{1}{4}, \frac{1}{2} + z) \quad (4) (\frac{1}{2} + x, \frac{1}{4}, \frac{1}{2} - z)$$

where the  $x$ ,  $y$  and  $z$  represent functional coordinates along the crystallographic  $a$ ,  $b$  and  $c$  directions, respectively. The results of the refinements are summarized in table 2.

We have determined the magnetic structure of the intermediate phase ( $T_C > T > T_i$ ) from the difference patterns corresponding to the magnetic contribution  $y_{\text{obs}}^{\text{mag}} = y_{\text{obs}}(T < T_C) - y_{\text{obs}}(T > T_C)$ , for the three compounds studied. All the peaks observed can be indexed with the crystallographic unit cell (propagation vector  $\mathbf{Q} = \mathbf{0}$ ), but new peaks appear at the positions forbidden by the  $Pnma$  selection rules, indicating that an antiferromagnetic component is present, leading to a non-collinear ferromagnetic structure. The best refinement corresponds to the arrangement of  $F_x C_z$ , using Bertaut's description [15]. The symbol  $F_x$  means a ferromagnetic ( $F_x = M_{1x} + M_{2x} + M_{3x} + M_{4x}$ ) alignment of the four Ho magnetic moments, while  $C_z$  is an antiferromagnetic one ( $C_z = M_{1z} + M_{2z} - M_{3z} - M_{4z}$ ). The magnetic moments are in the (4c) site positions, with components along the  $a$  and  $c$  crystallographic directions. In figure 7 is shown the arrangement of magnetic moments within the crystallographic unit cell. The present results lead to the values gathered in table 2. Using spherical coordinates ( $r, \theta, \phi$ ), the angles  $\theta$  are  $62.6^\circ$ ,  $64.3^\circ$  and  $59.0^\circ$  for  $x = 0, 0.2$  and  $0.6$  respectively, while  $\phi = 0$  for all the compounds. The magnetic structure of HoNi coincides quite well with that reported in [3] and [7].

From the analysis of the low-temperatures patterns (see figure 6) we can assert that the magnetic structures evolve towards a magnetic ordering having a ferromagnetic component along the  $b$  direction. The arrangement is then labelled as  $F_x F_y C_z$ . The best fitted profiles correspond to the values of the magnetic moment components summarized in table 2. From these values the angles  $\theta$  and  $\phi$  are  $64.7^\circ$  and  $24.0^\circ$  for  $x = 0$ ,  $64.3^\circ$  and  $13.6^\circ$  for  $x = 0.2$  and  $59.5^\circ$  and  $2^\circ$  for  $x = 0.6$ , respectively.

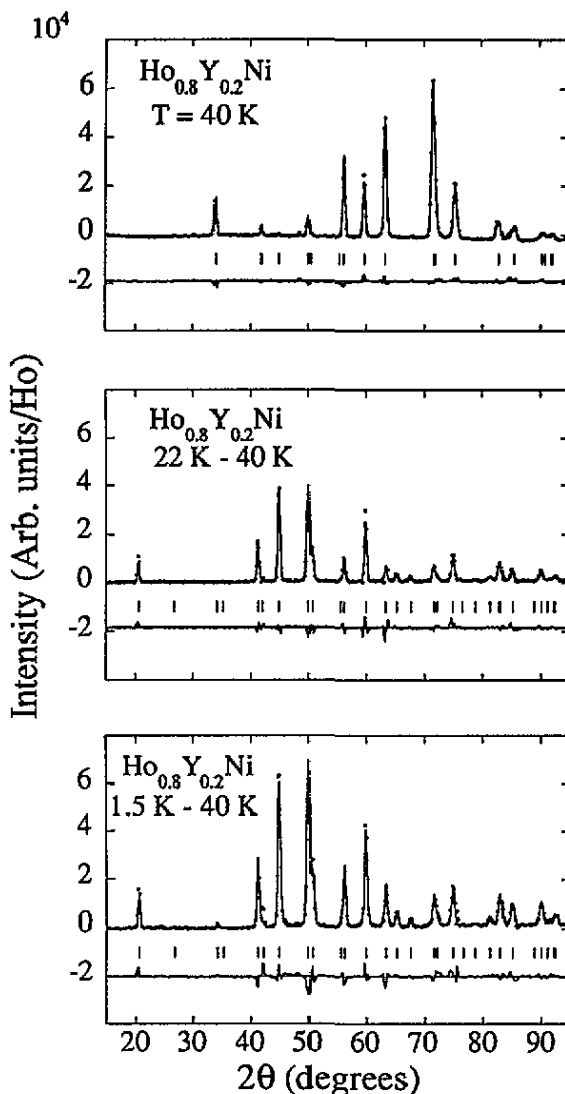
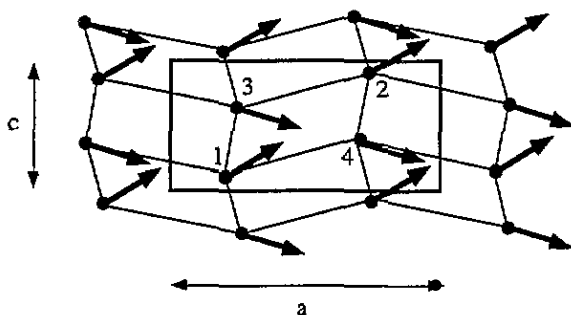


Figure 6. Neutron diffraction patterns in  $\text{Ho}_{0.8}\text{Y}_{0.2}\text{Ni}$ . At 40 K and for the difference patterns (22 – 40 K and 1.5 – 40 K): points are the observed counts and continuous line is the Rietveld refinement. The curve at the bottom of each figure is the difference pattern given by  $y_{\text{obs}} - y_{\text{cal}}$ ; the small vertical marks indicate the angular positions of the allowed Bragg reflections.

We have also studied the evolution of the structures with the temperature, recording diagrams at very close temperatures. We can then analyse the thermal dependence of the spherical angles  $\theta$  and  $\phi$  of the magnetic structures for the three compounds studied. It turns out that (i) the angle  $\theta$  seems to be temperature independent in all cases, (ii) the angle  $\phi$  depends much more on temperature: as shown in figure 8, the magnitude of  $\phi$  decreases with increasing yttrium content. In this figure, our results are also compared with those found using torque measurements and neutron diffraction on an  $\text{HoNi}$  single crystal [5, 7]. It is worth noting that some differences exist in the value of  $\phi$  in  $\text{HoNi}$  between the present measurements on a polycrystalline sample and the results obtained previously

**Table 2.** Structural and magnetic characteristics of  $\text{Ho}_{1-x}\text{Y}_x\text{Ni}$  compounds.  $M_x$ ,  $M_y$  and  $M_z$  are the magnetic moment components along the crystallographic  $a$ ,  $b$  and  $c$  directions, respectively.

	HoNi	$\text{Ho}_{0.8}\text{Y}_{0.2}\text{Ni}$	$\text{Ho}_{0.4}\text{Y}_{0.6}\text{Ni}$
Crystallographic structure	FeB type	FeB type	FeB type
Cell parameters			
$a$ (Å)	6.960	7.005	7.064
$b$ (Å)	4.126	4.112	4.100
$c$ (Å)	5.384	5.408	5.440
Atomic positions			
$x(\text{Ho or Y})$	0.173	0.182	0.182
$z(\text{Ho or Y})$	0.128	0.137	0.125
$x(\text{Ni})$	0.036	0.036	0.042
$z(\text{Ni})$	0.633	0.632	0.627
$R_{\text{nuclear}}$ (%)	7.7	6.4	8.5
Intermediate magnetic structure	$F_x C_z$	$F_x C_z$	$F_x C_z$
$M_x$ ( $\mu_B$ )	$6.28 \pm 0.06$	$5.83 \pm 0.07$	$5.88 \pm 0.09$
$M_y$ ( $\mu_B$ )	0	0	0
$M_z$ ( $\mu_B$ )	$3.26 \pm 0.05$	$2.81 \pm 0.04$	$3.53 \pm 0.08$
$R_{\text{mag}}$ (%)	13.4	13.3	13.2
Low-temperature magnetic structure	$F_x F_y C_z$	$F_x F_y C_z$	$F_x F_y C_z$
$M_x$ ( $\mu_B$ )	$7.06 \pm 0.07$	$7.61 \pm 0.06$	$7.29 \pm 0.09$
$M_y$ ( $\mu_B$ )	$3.14 \pm 0.14$	$1.84 \pm 0.19$	$0.27 \pm 0.18$
$M_z$ ( $\mu_B$ )	$3.66 \pm 0.06$	$3.77 \pm 0.05$	$4.29 \pm 0.07$
$R_{\text{mag}}$ (%)	14.6	14.2	16.0

**Figure 7.** A schematic representation in the  $ac$  plane of the magnetic structures observed in  $\text{Ho}_{1-x}\text{Y}_x\text{Ni}$  compounds. The magnetic arrangement corresponds to the  $F_x C_z$  magnetic mode. Atoms 1, 2, 3 and 4 are located at the positions indicated in the text.

on a single crystal, but not in the general trend of the thermal variation. In the same way, the thermal variation of the  $\text{Ho}^{3+}$  magnetic moment, obtained from neutron scattering, is similar for all the  $\text{Ho}_{1-x}\text{Y}_x\text{Ni}$  compounds and quite close to that exhibited in the HoNi single crystal. The maximum magnetic moments at 1.5 K are 8.55, 8.69 and  $8.46\mu_B$  for  $x = 0, 0.2$  and  $0.6$ , respectively (see table 2), while in the HoNi single crystal the value was about  $8.8\mu_B$  at 4.2 K [7]. All these experimental facts seem to indicate that the evolution of the magnetic structures in the same compound, as well as from one compound to another, originate mainly from the modification of the relative importance of the magnetocrystalline anisotropy and the exchange interactions. This modification induces changes in the easy magnetization direction, and will be discussed in the general discussion of this paper.



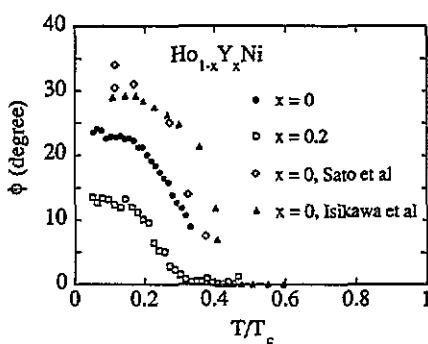


Figure 8. The thermal variation of the angle  $\phi$  for HoNi and Ho<sub>0.8</sub>Y<sub>0.2</sub>Ni. The data of Sato *et al* [5] were obtained from torque measurements, whereas those of Isikawa *et al* [7] were found from neutron diffraction on HoNi, both measurements in a single crystal of this material.

From the neutron thermodiffractograms collected for the three compounds  $x = 0, 0.2$  and  $0.6$ , between the paramagnetic phase and the lowest temperature measured,  $1.5$  K, we have studied the thermal dependence of the cell parameters of Ho<sub>1-x</sub>Y<sub>x</sub>Ni compounds. As well as the properties presented before, these dependences also show anomalies at  $T_C$  and  $T_t$ . In figures 9 and 10, we present the thermal variation of  $a$ ,  $b$ ,  $c$  and the cell volume for HoNi and Ho<sub>0.8</sub>Y<sub>0.2</sub>Ni compounds respectively. Some similarities could be stressed analysing the two figures together: (i) changes in the slope are observed in the vicinity of the corresponding temperatures,  $T_C$  and  $T_t$ , for both transitions; (ii) from the variation of the parameters on the paramagnetic range, we can ascertain the same lattice expansion behaviour for the two compounds, i.e.,  $a$  and  $c$  decrease with decreasing temperature while  $b$  increases.

However, striking features appear when we look at the magnetic effects that take place below the Curie temperature. In Ho<sub>0.8</sub>Y<sub>0.2</sub>Ni, the spontaneous magnetostriction reinforces the tendency of the lattice parameters and evolves gradually, as in a second-order transition, while in HoNi, it appears that the sign of the thermal expansion coefficient,  $\alpha_L = (1/L)(\partial L/\partial T)$  with  $L = a, b$  and  $c$ , changes abruptly in an interval of roughly  $5$  K around  $T_C$ , in the three directions. It seems that in this case the rise of the magnetic order acts against the lattice thermal variation tendency. For Ho<sub>0.4</sub>Y<sub>0.6</sub>Ni, only in the  $c$  direction, the influence of the magnetic order is clearly observed; this is probably due to the lower transition temperatures in this compound.

On the other hand, it is then likely that a close relationship between the thermal expansion behaviour along  $b$  ( $b$  increases at low temperatures), and the appearance of the magnetic component in this direction exist. However, the observed differences between the transitions at  $T_C$ , in HoNi and Ho<sub>0.8</sub>Y<sub>0.2</sub>Ni, needs a deeper study of the thermal expansion and the comparison with the magnetostriction behaviour of other isostructural compounds such as GdNi<sub>1-x</sub>Cu<sub>x</sub> [16], to ascertain the origin of such experimental evidence.

Finally, the cell volume of Ho<sub>1-x</sub>Y<sub>x</sub>Ni compounds increases with the yttrium content, as expected due to the larger volume of this ion with respect to that of the Ho<sup>3+</sup> ion.

## 5. Discussion

In the present work, it has been proved that the substitution of Ho atoms by Y clearly modifies the magnetic behaviour of the Ho<sub>1-x</sub>Y<sub>x</sub>Ni system. It turns out that this dilution

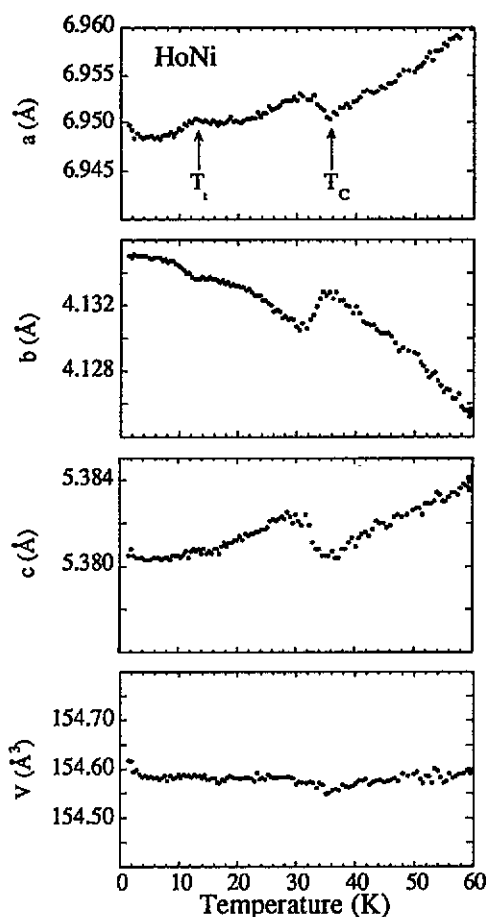


Figure 9. The thermal dependence of the cell parameters and volume of the  $\text{HoNi}$  compound.

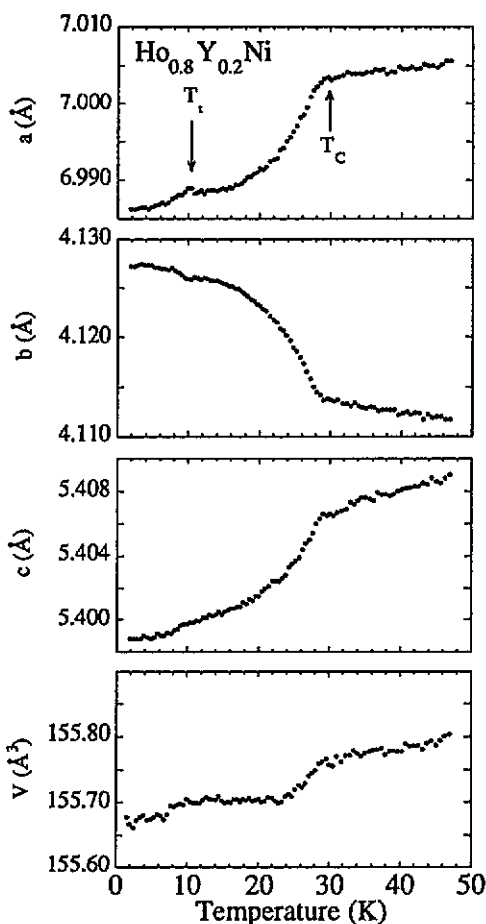


Figure 10. The thermal dependence of the cell parameters and volume of the  $\text{Ho}_{0.8}\text{Y}_{0.2}\text{Ni}$  compound.

influences not only the strength of magnetic interactions, leading to a decrease of  $T_C$ , but also the relationship between CEF and RKKY interactions, giving rise to changes in the magnetic structures observed below  $T_C$ . The magnetic structures obtained for  $\text{HoNi}$  agree quite well with those previously reported on a single crystal of this material [5, 7, 19]. The ferromagnetic non-collinear structure,  $F_x C_z$ , found in all the studied compounds just below  $T_C$ , is a common arrangement, when the magnetic ion is located in a low-symmetry site, as is the case of the (4c) site in the orthorhombic  $Pnma$  space group [4, 17]. As has been discussed for the equiatomic  $\text{RENi}$  compounds [18], this arrangement is imposed by the strong magnetocrystalline anisotropy. In fact, it can be  $F_x C_z$  or  $C_x F_z$  depending on the sign of the second-order Stevens constant  $\alpha_J$ , ( $\alpha_J < 0$  in Tb, Dy or Ho and  $\alpha_J > 0$  in Er and Tm).

However, below  $T_i$ , the magnetic structure changes towards another non-collinear ferromagnetic ordering, characterized by the mode  $F_x F_y C_z$ . Among all the  $\text{RENi}$  compounds,  $\text{HoNi}$  is the only one in which a change in the magnetic structure at low temperatures has been observed. The magnetic structure consists of two coupled modes,  $F_x C_z$  and  $F_y$ , belonging to two different irreducible representations of the  $Pnma$  space

group for  $Q = 0$  [15]. The existence of two different modes in the magnetic structure means that the role of the fourth- and sixth-order CEF parameters became more important at these temperatures, and the appearance of a ferromagnetic component along the  $b$  direction is not forbidden.

As can be seen in figure 4, the ordering temperatures,  $T_C$  and  $T_i$ , decrease almost linearly with increasing Y content, as corresponds to the reduction of the exchange interactions due to the dilution with non-magnetic Y ions. The same magnetic structures appear in all the compounds,  $F_xC_z$  between  $T_i < T < T_C$  and  $F_xF_yC_z$  for  $T < T_i$ . However, it is important to note that in the lower-temperature phase, the  $b$  component of the magnetic moment decreases with the yttrium content.

The facts allow us to interpret the magnetic evolution of these compounds in the following way: the decrease of the  $b$  component mentioned above means that the system tends to recover the magnetic  $F_xC_z$  structure at low temperatures when we decrease the magnetic exchange interactions by the introduction of Y ions. These exchange interactions becomes less important than the CEF effects, as is the case for HoNi and other RENi compounds just below  $T_C$ . An interesting additional point to this discussion could be provided by the behaviour of the isostructural  $GdNi_{0.7}Cu_{0.3}$  [9], without CEF effects, which presents the  $b$  direction as the easy magnetization axis.

Therefore, we can conclude that when CEF effects are preponderant the  $F_xC_z$  magnetic phase appears, but the magnetic interactions favour the magnetization along the  $b$  direction. The stability of one or other structure depends on the relative importance of CEF and exchange interactions.

Some comments could also be stressed about the nature of the energy levels of this system. In fact the relation  $T_i/T_C$  is almost constant through the series; this feature reflects the fact that the CEF interactions are quite similar in all the  $Ho_{1-x}Y_xNi$  compounds. Furthermore, due to the low symmetry of the (4c) site, the CEF completely splits the  $J = 8$  multiplet; the resulting  $2J + 1$  states are all non-magnetic singlets. It would be then expected in these conditions that  $T_C$  as a function of the yttrium content would vary quickly near the critical concentration  $x_c = 0.9$ , as observed in well known non-magnetic singlet ground state systems such as diluted  $Pr_xY_{1-x}Ni_2Si_2$  [20]. However this is not the case observed in our compounds, because the linear dependence of  $T_C$  on  $x$  is clearly reminiscent of systems with magnetic doublets as ground states. Taking into account all these arguments, we can deduce that for  $Ho_{1-x}Y_xNi$ , the lowest-energy levels are two singlets close to each other, so the system behaves as if there were a pseudomagnetic doublet. This fact is confirmed by the specific heat measurements [21], because the entropy at  $T_i$  is around  $10 \text{ J K}^{-1} \text{ mol}^{-1}$  and the involved CEF levels are then around three, it being these states that mainly govern the magnetic properties of the system at low temperatures.

This study on the magnetic properties and structures of the  $Ho_{1-x}Y_xNi$  procures then new aspects and evidence about how the magnetism of the RENi compounds is sensitive to the competition between CEF and RKKY interactions.

## Acknowledgments

This work was supported by the Comision Interministerial de Ciencia y Tecnología (grant MAT-93, 0691-C02-01).

## References

- [1] Walline R E and Wallace W E 1964 *J. Chem. Phys.* **41** 1587
- [2] Abrahams S C, Bernstein J L, Sherwood R C, Wernick J H and Williams H J 1964 *J. Phys. Chem. Solids* **25** 1069
- [3] Lemaire R and Paccard D 1970 *Les Elements des Terres Rares* vol 2 (Paris: CNRS) p 231
- [4] Gignoux D 1974 *J. Physique* **35** 455
- [5] Sato K, Isikawa Y and Mori K 1982 *J. Appl. Phys.* **53** 8222
- [6] Sato K, Iwasaki S, Mori K, Ohashi M and Yamaguchi Y 1983 *J. Magn. Magn. Mater.* **31-34** 207
- [7] Isikawa Y, Mori K, Sato K, Ohashi M and Yamaguchi Y 1984 *J. Appl. Phys.* **55** 2031
- [8] Mori K and Sato K 1980 *J. Phys. Soc. Japan* **49** 246
- [9] Blanco J A, Gomez Sal J C, Rodriguez Fernandez J, Gignoux D, Schmitt D and Rodriguez-Carvajal J 1992 *J. Phys.: Condens. Matter* **4** 8233
- [10] Gómez-Sal J C, Rodriguez Fernandez J, López Sánchez R J and Gignoux D 1986 *Solid State Commun.* **59** 771
- [11] Rao V U S and Wallace W E 1970 *Phys. Rev. B* **2** 4613
- [12] Blanco J A, Gignoux D, Gomez Sal J C, Rodriguez Fernandez J and Schmitt D 1992 *J. Magn. Magn. Mater.* **104-107** 1285
- [13] Rodriguez-Carvajal J, Anne M and Pannetier J 1987 *ILL Internal Report* 87RO14T
- [14] Rodriguez-Carvajal J 1990 *Abstracts Satellite Meeting on Powder Diffraction XV Congress IUCr (Toulouse, 1990)* p 127
- [15] Bertaut E F 1963 *Magnetism* vol III, ed G T Rado and H Shul (New York: Academic)
- [16] Espeso J I, Rodriguez Fernandez J, Gomez-Sal J C and Blanco J A 1994 *IEEE Trans Magn.* **MAG-30** 1009
- [17] Castets A, Gignoux D and Gómez Sal J C 1980 *J. Solid. State Chem.* **31** 197
- [18] Rossat-Mignod J and Tcheou F 1972 *J. Physique* **33** 423
- [19] Isikawa Y, Higashi K, Miyazaki T and Sato K 1983 *High Field Magnetism Proc. Symp. (Osaka)* (Amsterdam: North-Holland) p 101
- [20] Blanco J A, Gomez Sal J C and Schmitt D 1992 *J. Magn. Magn. Mater.* **116** 128
- [21] Sato K, Isikawa Y, Mori K and Miyazaki T 1990 *J. Appl. Phys.* **67** 5300